PERGAMON

Solid State Communications 115 (2000) 483–487

solid state communications

www.elsevier.com/locate/ssc

Solidus curve of the Al–Cu alloy system under pressure

H.-M. Kagaya*, T. Suzuki, M.-S. Takaya, T. Soma

Department of Computer Science and Engineering, Faculty of Engineering and Resource Science, Akita University, Akita 010-8502, Japan

Received 20 October 1999; accepted 5 May 2000 by D.E. Van Dyck

Abstract

The mean-square displacement of thermal vibrations and melting for the Al and Al–Cu alloy system are studied using our previous treatment based on microscopic electronic theory. The temperature- and concentration-dependent mean-square displacement for $Al_{1-x}Cu_x$ system decreases under pressure. The Debye temperature obtained at low temperatures for $Al_{1-x}Cu_x$ solid solution decreases as a function of the Cu atomic fraction x, but increases at higher temperatures. The effect of pressure on the solidus curve is discussed by applying Lindeman's melting law to the alloy system, and the phase diagram of Al–Cu alloy system under pressure is predicted theoretically. © 2000 Elsevier Science Ltd. All rights reserved.

Keywords: A. Metals; D. Anharmonicity; D. Phase transitions; D. Phonons; D. Thermodynamic properties

1. Introduction

Since the increase of Si and Ge solubility in Al was found [1,2] under pressure by rapid quenching from the liquid state, the physical properties of Al-rich alloy systems have been an interesting field experimentally and theoretically. Previously, we have studied the solid solubility of Si, Ge [3] and Cu [4] in Al under pressure and the mechanical properties. Then, considering the volume and electron density effect on the lattice dynamics of the pure constituent atom, we have studied quantitatively the lattice dynamics [5] and thermal properties [6] of Al–Cu alloy system.

The intensity of the scattered wave from a crystal lattice is observed to be temperature-dependent and varies exponentially from its value at absolute zero. This temperature dependent exponential factor is known as the Debye–Waller factor and is related to the mean-square displacements of the constituent atoms in the crystal. As the temperature rises, the root-mean-square displacement becomes large, and the contributions to the free energy from the anharmonic term produce the thermal expansion. The increase of the root-mean-square displacement at higher temperatures brings about fusion of the solid lattice by Lindeman's melting law [7]. Therefore, the mean-square displacement is an important measure related to the anharmonic and melting properties. Previously some experimental studies [8–10] about the mean-square displacements of pure Al from the X-ray Debye–Waller factor have been reported. Then, the pressure effect on the melting temperature of Al at low pressure regions has also been obtained experimentally [11,12]. On the other hand, theoretical studies (for example, see [13,14]) about the Debye–Waller factor and the melting of Al have been reported, but their obtained results were not conclusive, especially in the phenomenological treatment and in the quantitative stage. In the present work, we calculate the temperature dependence of the mean-square displacement for pure Al and Al–Cu solid solution using our previous treatment [5,6]. Then, using the pressure-dependent mean-square displacement and Lindeman's melting law [7], we study the compression effect on the melting point of Al and the solidus curve of Al–Cu alloy system.

2. Formulations

When the substitutional $Al_{1-x}Cu_x$ solid solution is formed, Al or Cu atoms in the solid solution are in a state of volume and electron density change in comparison with those in pure Al or Cu. Therefore, we consider apparently the lattice vibration of Al or Cu atoms in the solid solution as that in pure Al or Cu crystal at the equilibrium atomic volume Ω_0 [4] and electron density $n = Z/\Omega_0$ of the solid solution with f.c.c. phase. The normal vibrational frequency $\nu_j^i(q, x)$ for the band (Al) and local (Cu) mode with atomic fraction x, branch j and wave vector q are determined by solving the secular equation with dynamical matrix [5].

* Corresponding author.

PII: S0038-1098(00)00225-8

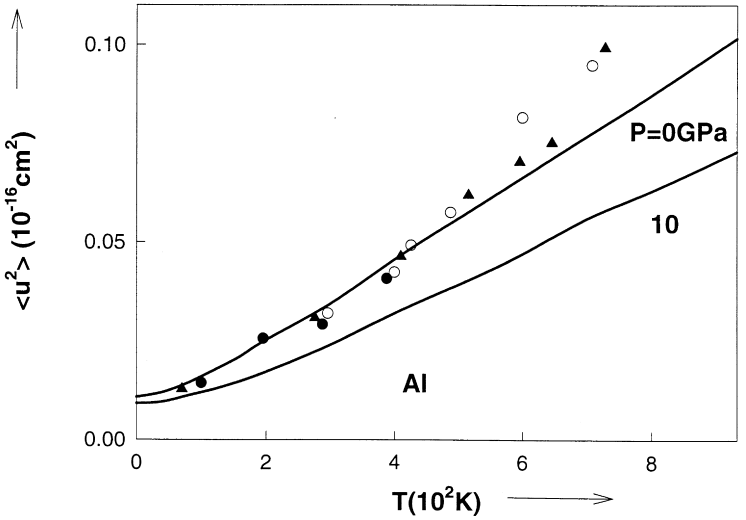

Fig. 1. The temperature-dependent mean-square displacement $\langle u^2\rangle$ under atmospheric pressure ($P \simeq 0$) and 10 GPa for pure Al. The points are experimental data such as ▲ [8], ○ [9] and ● [10].

The mean-square displacement $\langle u^2\rangle$ is temperature-dependent and is expressed in terms of the jth phonon mode with wave vector q and frequency $\nu_j(q)$ for a monoatomic cubic crystals as

$$\langle u^2\rangle = \frac{\mathrm{h}}{NM}\sum_{j,q}\frac{1}{\nu_j(q)}\left\{n[\nu_j(q)] + \frac{1}{2}\right\} \tag{1}$$

where $n[\nu_j(q)]$ is the Bose–Einstein occupation number. Then, the summation in Eq. (1) is over all the $N(q)$-points in the Brillouin zone and three j-branches of the phonon curves $\nu_j(q)$. In Debye's model, the mean-square displacement $\langle u^2\rangle$ is expressed with the use of Debye temperature θ as (for example, see [15])

$$\langle u^2\rangle = \frac{9\hbar^2}{4M\mathrm{k}\theta} \qquad \text{for } T \ll \theta \tag{2}$$

or

$$\langle u^2\rangle = \frac{9\hbar^2 T}{M\mathrm{k}\theta^2} \qquad \text{for } T > \theta. \tag{3}$$

Lindeman [7] proposed that the melting process occurs when the root-mean-square displacement of the lattice vibration $\sqrt{\langle u^2\rangle}$ reaches a critical fraction of the nearest-neighbour distance. He assumed that this critical fraction was the same for all crystals, but it was later shown (for example, see [16,17]) that in various cubic metals and alkali halides this fraction was actually not constant. We define Lindeman's criterion for melting x_m as the ratio of two times the root-mean-square displacement at the melting point to the nearest-neighbour distance $R_1(=\sqrt{2}a/2)$ given by

$$x_\mathrm{m} = \frac{2\sqrt{\langle u^2\rangle}}{R_1}. \tag{4}$$

Considering the compression-dependence of the mean-square displacement $\langle u^2\rangle$ and the nearest-neighbour distance at a constant criterion for melting x_m, we can calculate the compression effect on the melting point by satisfying

$$x_\mathrm{m} = 2\sqrt{\langle u^2\rangle_{T_\mathrm{m}(P)}}/R_1(P) \tag{5}$$

and

$$R_1(P) = \left(\frac{\Omega}{\Omega_0}\right)^{1/3} R_1(\Omega_0) \tag{6}$$

where Ω_0 and Ω are the atomic crystal volume under atmospheric pressure ($P \simeq 0$) and pressure P, respectively.

The extension from pure Al to the Al–Cu alloy are done as follows. Using the band and local mode frequencies $\nu_j^i(q,x)$ [5] in the $Al_{1-x}Cu_x$ solid solution, the mean-square displacement $\langle u^2\rangle_x$ for this alloy system is given by

$$\langle u^2\rangle_x = (1-x)\frac{\mathrm{h}}{NM^{\mathrm{Al}}}\sum_{j,q}\frac{1}{\nu_j^{\mathrm{Al}}(q,x)}\left\{n[\nu_j^{\mathrm{Al}}(q,x)] + \frac{1}{2}\right\} + x\frac{1}{NM^{\mathrm{Cu}}}\sum_{j,q}\frac{1}{\nu_j^{\mathrm{Cu}}(q,x)}\left\{n[\nu_j^{\mathrm{Cu}}(q,x)] + \frac{1}{2}\right\}. \tag{7}$$

Using the concentration-dependent mean-square displacement $\langle u^2\rangle_x$ in Eq. (7), we define Lindeman's criterion for melting $x_\mathrm{m}(x)$ of this alloy as the ratio of two times the root-mean-square $\sqrt{\langle u^2\rangle_x}$ at the corresponding temperature on the solidus curve [1] under atmospheric pressure to the nearest-neighbour distance $R_1(x)(=\sqrt{2}a(x)/2)$ given by

$$x_\mathrm{m}(x) = \frac{2\sqrt{\langle u^2\rangle_x}}{R_1(x)}. \tag{8}$$

where $a(x)$ is the equilibrium lattice constant and related

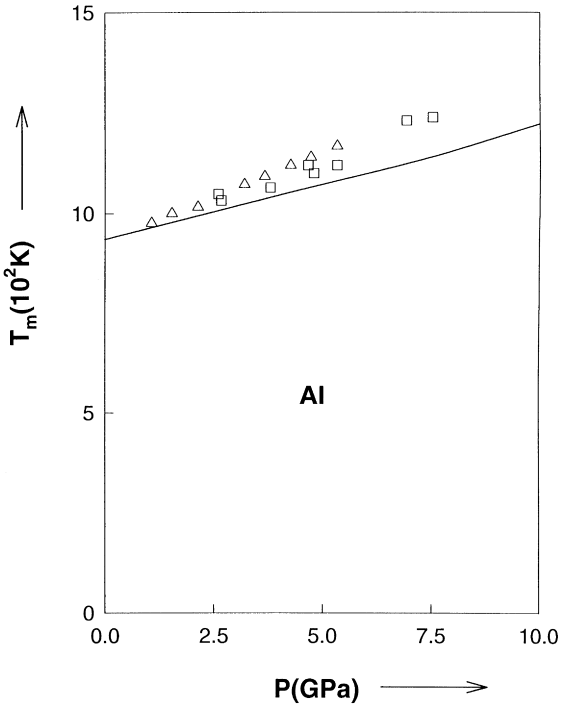

Fig. 2. The pressure-dependence of melting point T_m of pure Al. The points are experimental data: △ [11] and □ [12].

to the equilibrium crystal volume $\Omega(x)$ [4] by $a(x) = \{4\Omega(x)\}^{1/3}$. Using the compression-dependence of the mean-square displacement $\langle u^2\rangle_x$ and the nearest-neighbour distance $R_1(x)$ at a constant criterion for melting $x_m(x)$ in Eq. (8), we can calculate the compression effect on the solidus curve for the $Al_{1-x}Cu_x$ solid solution by satisfying

$$x_m = 2\sqrt{\langle u^2\rangle_{x,T_m(x,P)}}/R_1(x,P) \tag{9}$$

and

$$R_1(x,P) = \left\{\frac{\Omega(x)}{\Omega_0(x)}\right\}^{1/3} R_1(x,\Omega_0) \tag{10}$$

where the conversion from the pressure $P(x)$ to the compressed volume $\Omega(x)$ is performed using the equation of state [4] for this alloy system.

3. Numerical results and discussion

In numerical calculations of Eqs. (1) and (7), the wave vector q in the reciprocal space has been divided into 16 equal parts to give a grid of 4096 equally spaced points inside the first Brillouin zone. Considering the symmetry of the Brillouin zone, it is sufficient to determine the phonon frequencies in the range

$$q = \frac{2\pi}{a}\frac{1}{16}(q_x, q_y, q_z) \tag{11}$$

where q_x, q_y, q_z are positive integers and satisfy the following inequalities such as $0 \le q_x \le q_y \le q_z \le 16$ and $q_x + q_y + q_z \le 24$. There are 149 points in the irreducible 1/48 th part of the Brillouin zone. A divergence occurs for the $q \simeq 0$ acoustical mode phonons in the sum over the wave vector mesh of Eqs. (1) and (7). Therefore, the contribution to the mean-square displacement owing to $q \simeq 0$ acoustical mode frequencies is calculated by converting the summation to an integral and assuming a Debye distribution over the

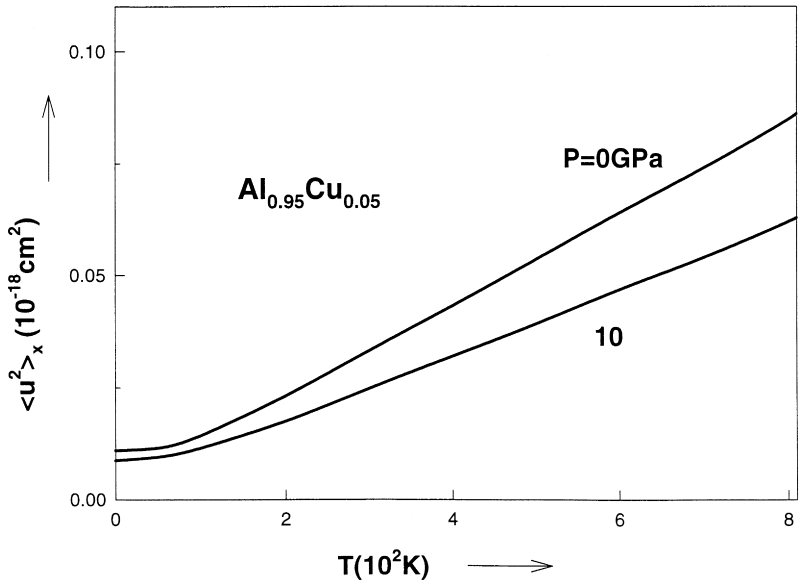

Fig. 3. The temperature-dependent mean-square displacement $\langle u^2\rangle_x$ under $P = 0$ and 10 GPa for $Al_{0.95}Cu_{0.05}$ solid solution.

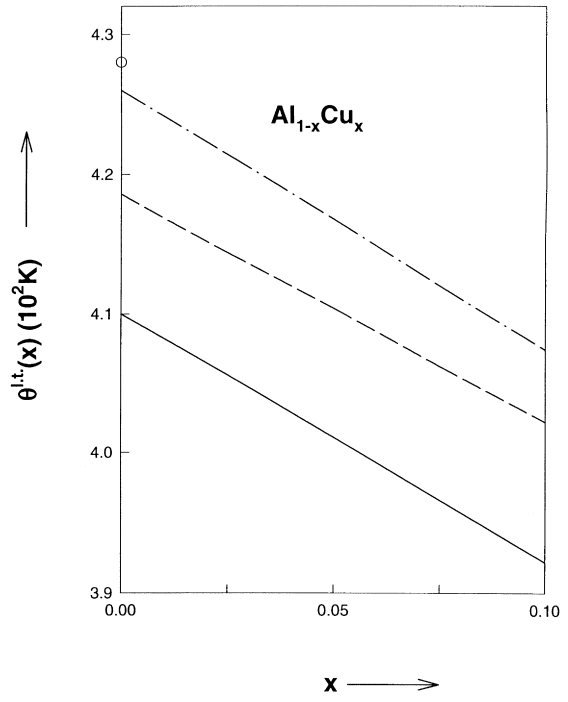

Fig. 4. The concentration-dependence of Debye temperature $\theta^{\text{l.t.}}$ $T = 0$ K for $Al_{1-x}Cu_x$ solid solution (Full line). Broken and chain curves are those [6] estimated from the specific heat and from the mean elastic velocity. The point for pure Al is the observed data [20] from elastic velocity.

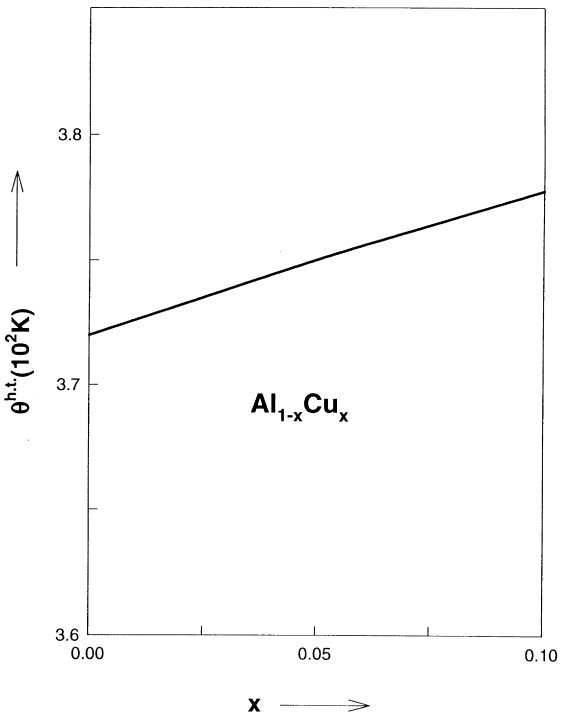

Fig. 5. The concentration-dependence of Debye temperature $\theta^{\text{h.t.}}$ at 820 K for $Al_{1-x}Cu_x$ solid solution.

volume of integration which is assumed to be 1/4096 th of the total Brillouin zone volume (for example, see [18,19]).

First, the temperature dependence of $\langle u^2 \rangle$ under atmospheric pressure ($P \simeq 0$) and 10 GPa for pure Al using Eq. (1) are shown in Fig. 1, where points are experimental data [8–10] and T_m the melting point at atmospheric pressure. In Fig. 1 and what follows, the results with Vashishta–Singwi dielectric function [3] are given, and the variation width of the obtained results using different forms of exchange and correlation [3] are within 1.0% at the absolute zero and 2.1% at T_m. The obtained data of the critical fraction for melting x_m in Eq. (4) is 0.2216 ± 0.0005 for pure Al. Then, the obtained results for the pressure dependence of the melting point for Al satisfying Eq. (5) are shown in Fig. 2, where the maximum deviation of the melting point obtained due to other screening functions [3] is within 0.5% and the points the experimental data [11,12]. From Fig. 2, we see that the melting point of pure Al increases under compression consistent with the experimental data [11,12].

Secondly, using the band and local mode frequencies $\nu_j^i(q,x)$ [5] in the $Al_{1-x}Cu_x$ alloy system, the temperature dependence of the mean-square displacement $\langle u^2 \rangle_x$ for the $Al_{0.95}Cu_{0.05}$ solid solution obtained using Eq. (7) is shown in Fig. 3. From Fig. 3, we see that the pressure effect on the mean-square displacement for this alloy system is similar to that for pure Al in Fig. 1. Then, we calculate the Debye temperature $\theta^{\text{l.t.}}$ and $\theta^{\text{h.t.}}$ at lower and higher temperatures using Eqs. (2) and (3). The obtained concentration x-dependence of the Debye temperature $\theta^{\text{l.t.}}$ at the absolute zero and $\theta^{\text{h.t.}}$ at the representative temperature such as 820 K for $Al_{1-x}Cu_x$ system are shown in Figs. 4 and 5, where the maximum deviation of the Debye temperature obtained due to other screening functions [3] is within 1% and the obtained data of $\theta^{\text{l.t.}}$ for pure Al is in good agreement with the experimental data [20] from elastic velocity. The relative difference of the Debye temperature $\Delta\theta(x) \equiv \theta(x) - \theta(x=0)$ from that for pure Al have a reduced accuracy $|\Delta\theta(x)/\theta(x)| \leq 0.5\%$ due to other screening functions [3]. From Figs. 4 and 5, we see that the Debye temperature decreases with the solubility of Cu at low temperatures, but increases at high temperatures. The concentration-dependence of the Debye temperature $\theta^{\text{l.t.}}(x)$ at absolute zero for $Al_{1-x}Cu_x$ alloy system in Fig. 4 is consistent with those [6] from the mean elastic velocity and from the specific heat.

Finally, we study the compression effect on the phase diagrams of the $Al_{1-x}Cu_x$ alloy system. The obtained solidus curves under pressure by satisfying Eq. (9) for the $Al_{1-x}Cu_x$ alloy system are shown in Fig. 6. Our obtained solidus curves in Fig. 6 have a calculated accuracy corresponding to $|\Delta x| \leq 0.01$ and $|\Delta T| \leq 5$ K. From Fig. 6, we predict that the solid solubility of Cu in Al is increased under pressure,

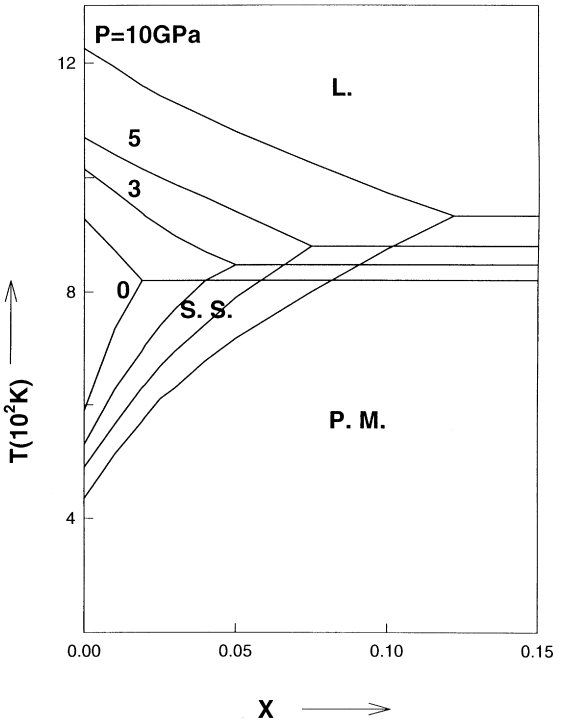

Fig. 6. The obtained phase diagram (absolute temperature T versus Cu atomic fraction x) under pressure $P = 0, 3, 5, 10$ GPa for Al-rich $Al_{1-x}Cu_x$ alloy system. The phase boundary between the liquid (L) and the solid solution (SS) or the phase mixture (PM) are obtained from the present study. The phase boundaries between SS and PM are from our previous study [4].

and we hope that there will be further experimental research in this field. The numerical calculations were carried out with the ACOS 3900 operating system in the Computer Center of Tohoku University.

References

[1] H. Mii, M. Senoo, I. Fujishiro, Jap. J. Appl. Phys. 15 (1976) 777.
[2] V.F. Degtyareva, G.V. Chipenko, I.T. Belash, O.I. Barkalov, E.G. Ponyatovskii, Phys. Status Solidi A 89 (1985) K127.
[3] T. Soma, Y. Funayama, H.-M. Kagaya, Solid State Commun. 77 (1991) 149.
[4] T. Soma, M. Ishizuka, H.-M. Kagaya, Solid State Commun. 95 (1995) 479.
[5] H.-M Kagaya, I. Kitabatake, T. Soma, Solid State Commun. 92 (1994) 365.
[6] H.-M. Kagaya, E. Serita, M. Sato, T. Soma, Solid State Commun. 100 (1996) 727.
[7] Z. Lindeman, Z. Phys. 11 (1910) 609.
[8] E.A. Owen, R.W. Williams, Proc. Roy. Soc. (London) A188 (1947) 509.
[9] D.R. Chipman, J. Appl. Phys. 31 (1960) 2012.
[10] P.A. Flinn, C.M. McManus, Phys. Rev. 132 (1963) 2458.
[11] A. Jayaraman, W. Klement, R.C. Newton, G.C. Kennedy, J. Phys. Chem. Solids 24 (1963) 7.
[12] J.F. Cannon, J. Phys. Chem. Ref. Data 3 (1974) 781.
[13] E.V. Zarochentsev, S.P. Krar-Chuk, T.M. Tarusina, Soviet Phys—Solid State 18 (1976) 239.
[14] A.P.G. Kutty, S.N. Vaidya, J. Phys. Chem. Solids 41 (1980) 1163.
[15] J.M. Ziman, Principles of the Theory of Solids, 2nd Edition, Cambridge University Press, Cambridge, 1976 (chap. 2).
[16] A.K. Singh, P.K. Sharma, Can. J. Phys. 46 (1968) 1677.
[17] J.S. Reid, T. Smith, J. Phys. Chem. Solids 31 (1970) 2689.
[18] J.F. Vetelino, S.P. Gaur, S.S. Mitra, Phys. Rev. B 5 (1972) 2360.
[19] D.N. Talwar, B.K. Agrawal, J. Phys. C 7 (1974) 2981.
[20] C. Kittel, Introduction to Solid State Physics, 6th Edition, Wiley, New York, 1986 (chap. 5).